

Electronic supplementary information

Investigation from chemical structure to photoluminescent mechanism: a type of carbon dots from pyrolysis of citric acid and an amine

*Yubin Song, Shoujun Zhu, Shitong Zhang, Yu Fu, Xiaohuan Zhao, Li Wang and Bai Yang**

State Key Laboratory of Supramolecular Structure and Materials, Jilin University, Changchun, P. R. China

byangchem@jlu.edu.cn

Table of contents in Electronic supplementary information:

- 1 Details on optimal CDs synthesis conditions.
- 2 Scheme S1 The process of forming the molecule (IPCA) and carbon dots.
- 3 Table S1 The elemental analysis results table.
- 4 Figure S1 The Abs, QY and Dep value of CDs solution.
- 5 Figure S2 The absorbance spectra of CDs synthesized in different temperature.
- 6 Figure S3 The 2D-NMR spectra of IPCA.
- 7 Figure S4 The characterization of product from refluxing methods.
- 8 Figure S5 ¹H-NMR spectrum and PL spectra of IPCA purified by extraction.
- 9 Figure S6 The PL intensity of IPCA/CDs after UV exposure.
- 10 Figure S7 The PL and Abs spectra of modified CDs.
- 11 Figure S8 PL stability of modified CDs.
- 12 Figure S9 The ¹H-NMR characterization of Et-CDs.
- 13 Figure S10 The characterization of 5 batches.
- 14 Figure S11 MS of CDs-140.
- 15 Figure S12 MS of CDs-200.
- 16 Figure S13 TEM image of the carbon core of CDs.
- 17 Figure S14 AFM image of the carbon core of CDs.
- 18 Figure S15 The PL lifetime measurement of batch 4 and batch 1.
- 19 Figure S16 The TEM image and PL spectra of carbon core.
- 20 Figure S17 The PL and PL lifetime characterization of carbon core.
- 21 Figure S18 The PL spectra of IPCA after hydrothermal treatment.
- 22 Figure S19 PL spectra of Et-CDs solution synthesized in 200 °C condition.
- 23 Figure S20 The characterization of PPCA.
- 24 Bio-application of IPCA and figure S21.
- 25 References in the ESI.

Details on optimal CDs synthesis conditions

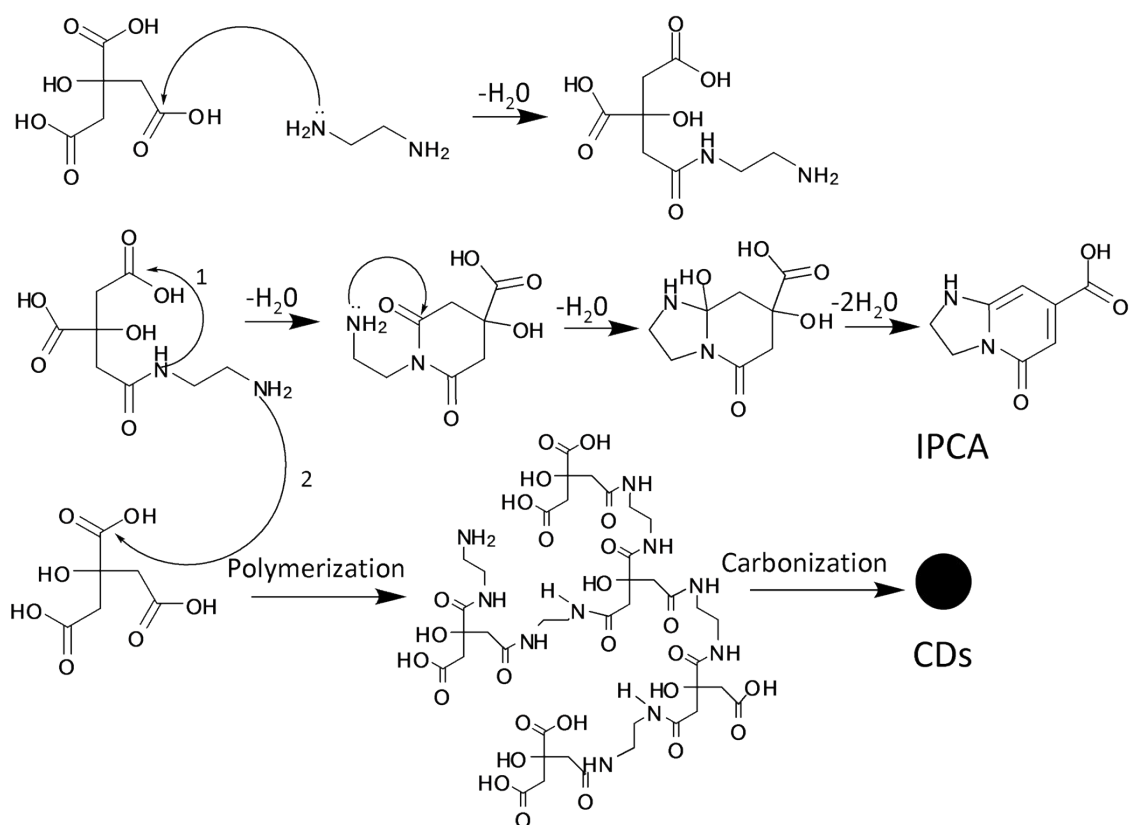
To develop our previous work, we further optimized the synthetic conditions. Herein, the influence factors of the hydrothermal process were investigated in detail.

We tested the CDs solution with different synthesis conditions: initial starting material ratios (short for value R), initial pH value and hydrothermal temperature. The input amount of starting material was reduced to obtain pure CDs (5 mmol: 5 mmol, in our previous work), for making sure the reagents undergo complete reaction. We fixed the concentration of one reagent as 1 mmol in 10 mL. For example, ratio 4 meant the initial amount of CA and EDA were 4 mmol and 1 mmol respectively. Ratio 0.333 meant the initial amount of CA and EDA is 1 mmol and 3 mmol respectively. The hydrothermal temperature was fixed as 200 °C, since both IPCA and nanodots appeared in this condition. The initial pH value can be tuned with sodium hydrate or hydrochloric acid for contrast experiments.

We considered three values to qualify the CDs here, the absorbance intensity (Abs), quantum yield (QY) and λ_{ex} dependence (Dep). The absorbance peak of IPCA was near 340 nm. However, CA and EDA possess no absorbance there. The Abs value of different samples was measured at 340 nm of the fixed concentration (300 times dilution of the original CDs solution directly from the reactors after hydrothermal reaction). Higher Abs value indicated more product contained in the solution. QY was measured through a relative method with quinine sulfate as reference. (Equation 1) The QY implied the efficiency of PL. Dep was a value defined in this work to qualify the λ_{ex} dependence PL behaviors. In stead of showing the PL spectra of different excitations (EX), we just presented a value. This value was the ratio between the PL intensities of 360 nm EX and 440 nm EX (Equation 2). Since the molecular state resulted in 443 nm emission with 360 nm EX, while carbon core state resulted in around 500 nm emission with 440 nm EX. This value indicated the ratio of the two states. If the spectrum was of none λ_{ex} dependence, this value should be extremely low. In contrast, the λ_{ex} dependent spectrum possessed high Dep value.

$$\begin{aligned} \text{Equations :} \quad \text{QY} &= \text{QY}_{\text{st}} * (\text{I}_x / \text{I}_{\text{st}}) * (\text{A}_{\text{st}} / \text{A}_x) & 1 \\ \text{Dep} &= \text{I}_{440 \text{ EX}} / \text{I}_{360 \text{ EX}} & 2 \end{aligned}$$

Note : In equation 1, “I” is the measured integrated emission intensity, and “A” is the optical density. The subscript "st" refers to standard with known QY and "x" for the sample. Quinine sulfate (0.1M H₂SO₄ as solvent; QY=0.54) was chosen as standard. In equation 2, “I” refers to the PL intensities of different EX.



Scheme S1 The assumed process of forming the molecule (IPCA), polymer cluster and carbon core form CA and EDA.

Note: Carbon nano structure can also derive from the pyrolysis of citric acid², which is not shown in the scheme.

Table S1 The elemental analysis results table.

	N	C	H	O	C/N
IPCA (In theory)	15.55	53.33	4.48	26.64	3.43
Sample from column separation					
batch 1	12.88	46.10	5.20	35.82	3.58
batch 2	12.57	45.28	5.12	37.03	3.60
batch 3	11.01	38.70	5.99	44.30	3.51
batch 4	10.43	35.06	5.09	49.42	3.36
CDs of different start material ratios (CA:EDA)					
4:1	5.19	45.97	5.49	43.35	8.86
2:1	9.94	49.46	5.62	34.98	4.98
1:1	11.14	40.17	5.66	43.03	3.61
1:2	14.88	35.43	7.25	42.44	2.38
1:4	15.17	31.83	7.74	45.26	2.10

Note: Due to the polarity groups on IPCA or CDs, water may be hard to exclude totally. Assessing the weight ratio of carbon and nitrogen (C/N) can avoid the influence of water.

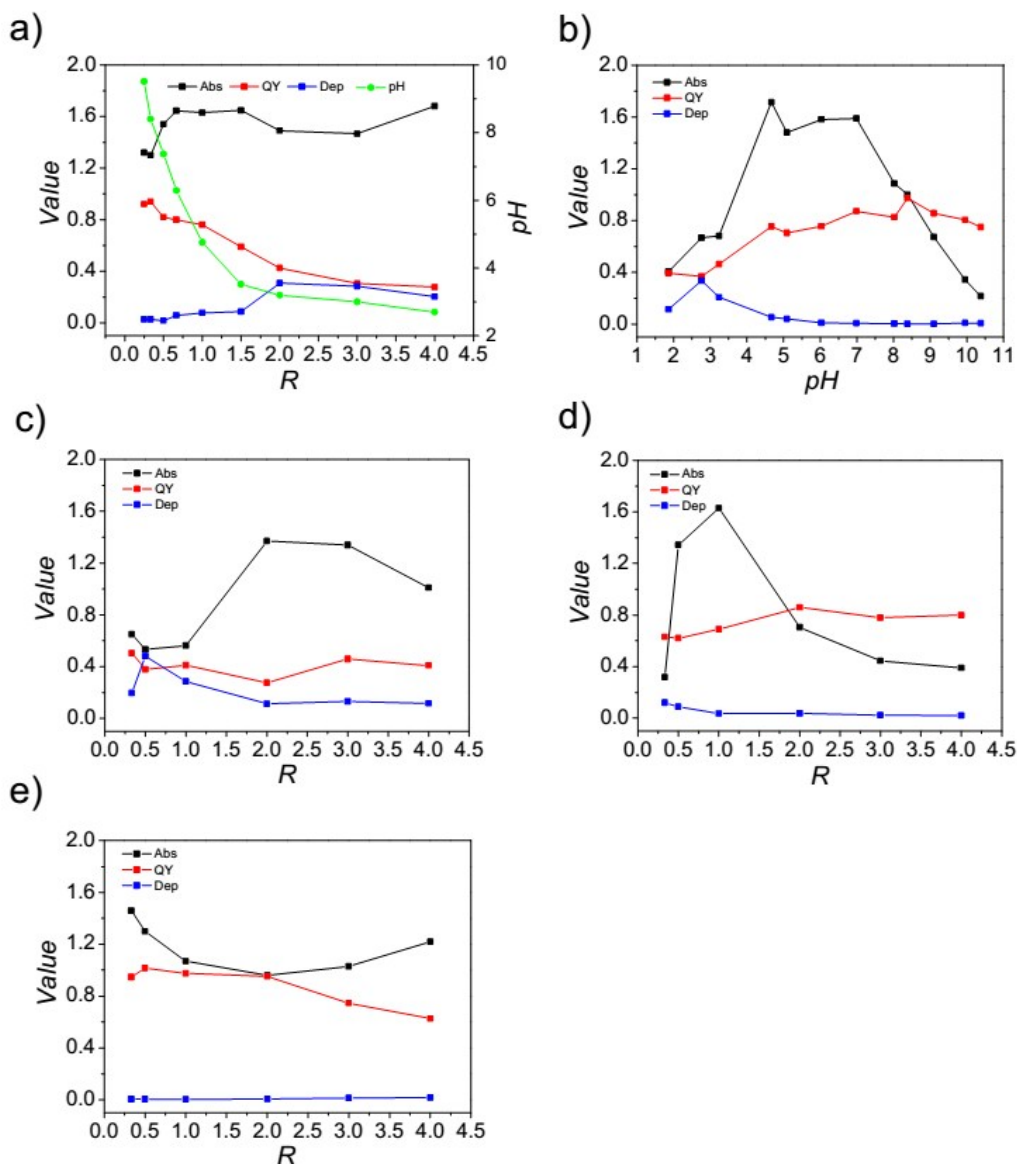


Figure S1 The Abs, QY and Dep value of CDs solution. a) CDs solution of different starting material ratios, b) CDs solution of different initial pH values while keeping R as 1 ,c-e) CDs solution of different starting material ratios, while keeping initial pH value as c) 3.0, d) 4.8 and e) 8.4.

Note : The CDs' properties of different R of CA and EDA was estimated in Figure S1 a. On one hand, the value R influenced the final composition of the product (Table S1). On the other hand, it changed the initial pH value of the system. The according pH values of different R were also presented in Figure S1a (green line). Then, the influence of initial pH value was investigated with keeping R as 1 (Figure S1 b). At last, the properties were assessed for CDs of the different value R with pH value controlled (Figure S1 c-e).

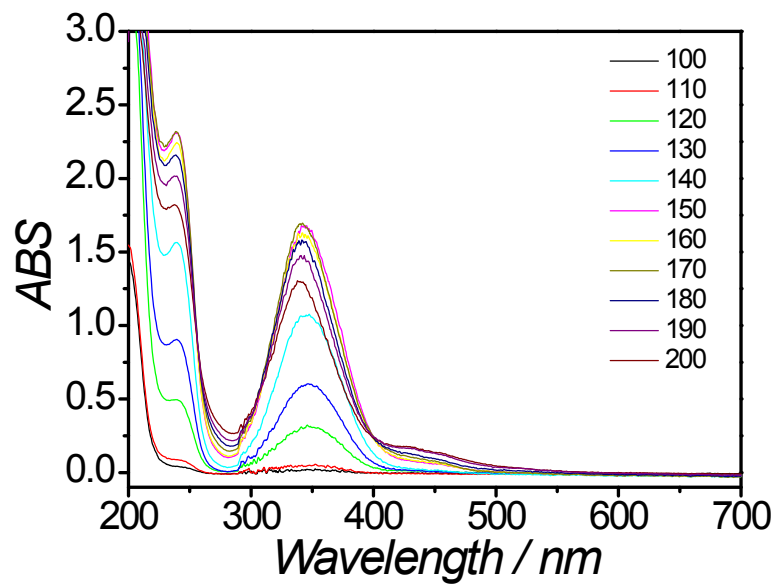


Figure S2 The absorbance spectra of CDs synthesized in different temperatures.

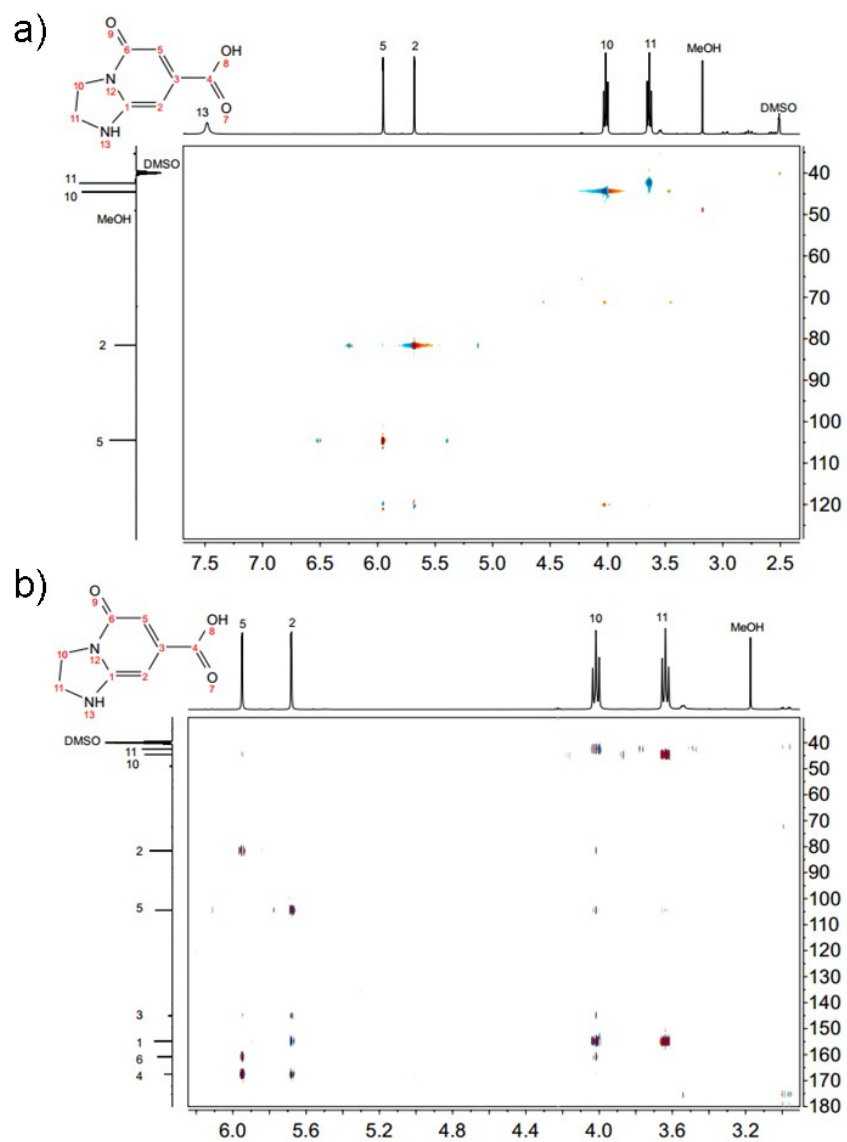


Figure S3 The 2D-NMR spectra of IPCA: HMQC a) and HMBC b).

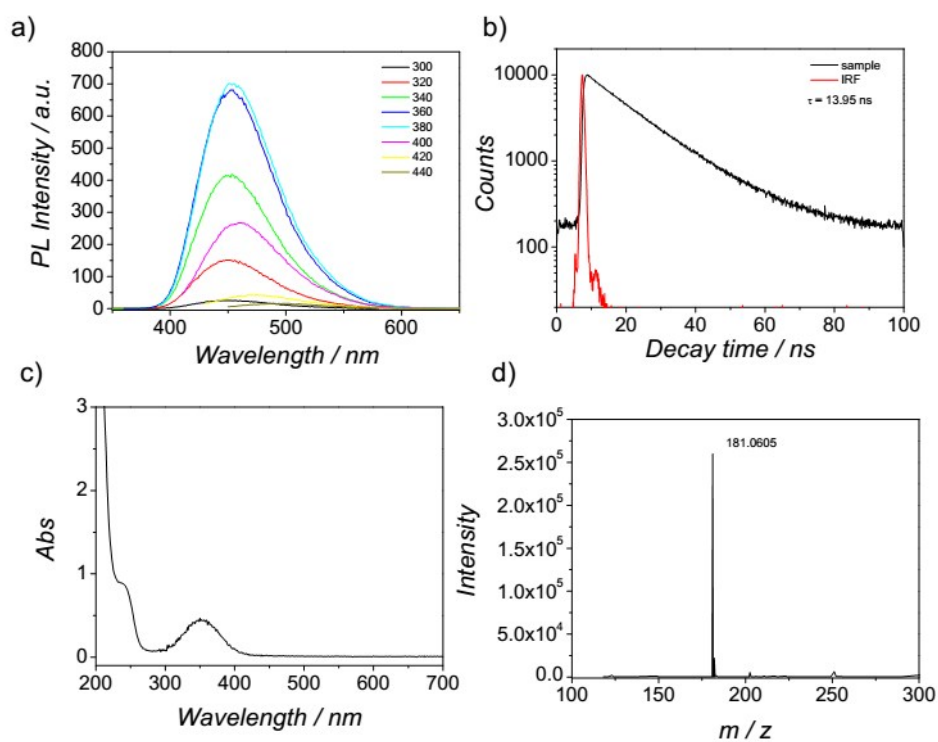


Figure S4 The characterization of product from refluxing methods. a) PL spectra, b) PL lifetime measurement, c) UV-vis absorption spectrum and d) ESI mass spectra.

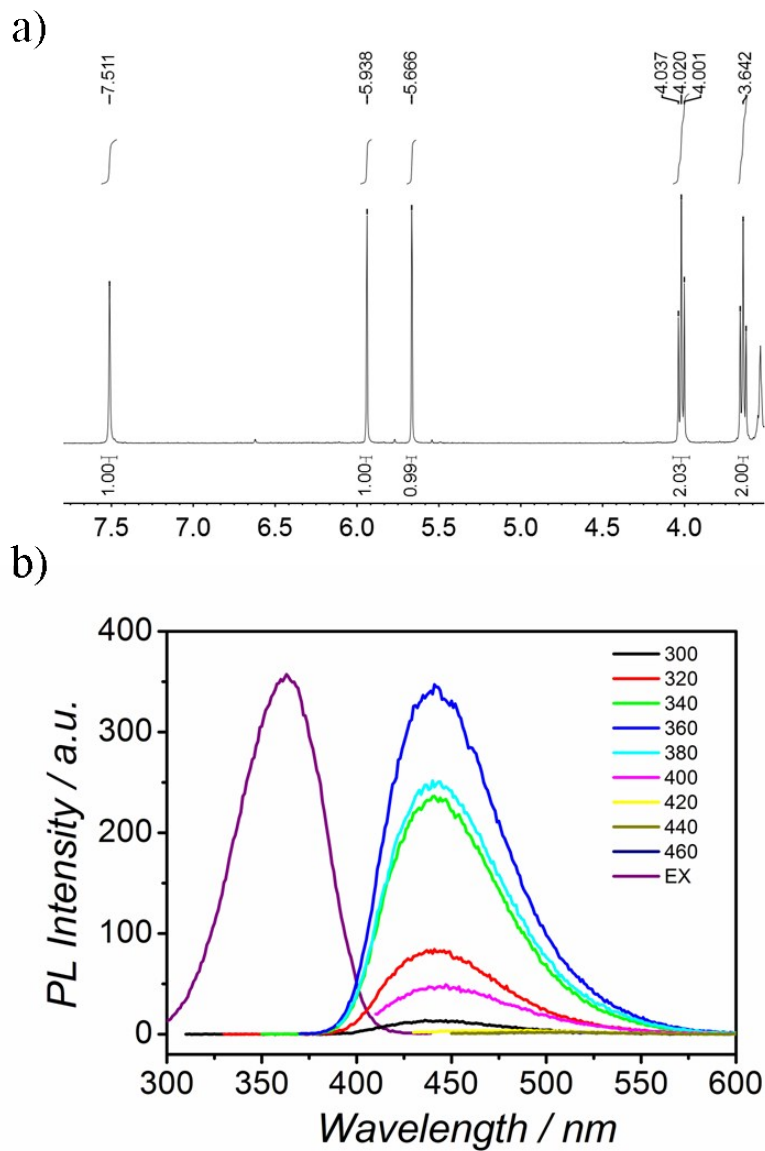


Figure S5 a) $^1\text{H-NMR}$ spectrum and b) PL spectra of IPCA purified by extraction.

Note: The absolute quantum yield was 82.6% and the PL lifetime was 14.04 ns, which were according with that of IPCA purified form column on silica.

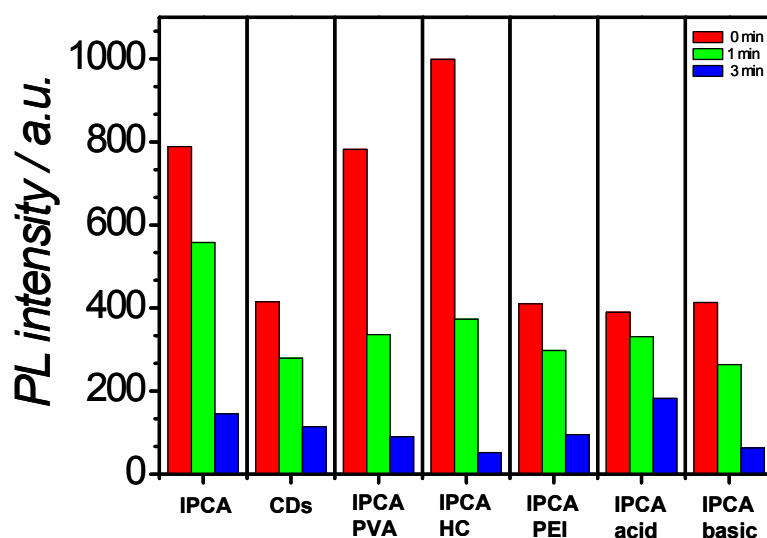


Figure S6 The PL of intensity IPCA/CDs after 2000 W UV exposure of different time.

Note: Group 1: only IPCA; Group 2: only CDs (Containing IPCA and carbon core), Group 3: IPCA with polyvinyl alcohol (20 mg/mL); Group 4: IPCA with hydroxyethyl cellulose (20 mg/mL); Group 5: IPCA with polyethyleneimine (weight ratio 2%, pH=10.22); Group 6: IPCA in acid condition (pH=3), Group 7: IPCA in basic condition (pH=11). After UV exposure, these solutions were excited by 360 nm light, and their PL intensity at the PL peak was recorded on the spectrophotometer. The final concentration of IPCA/CDs was 0.01 mg/mL.

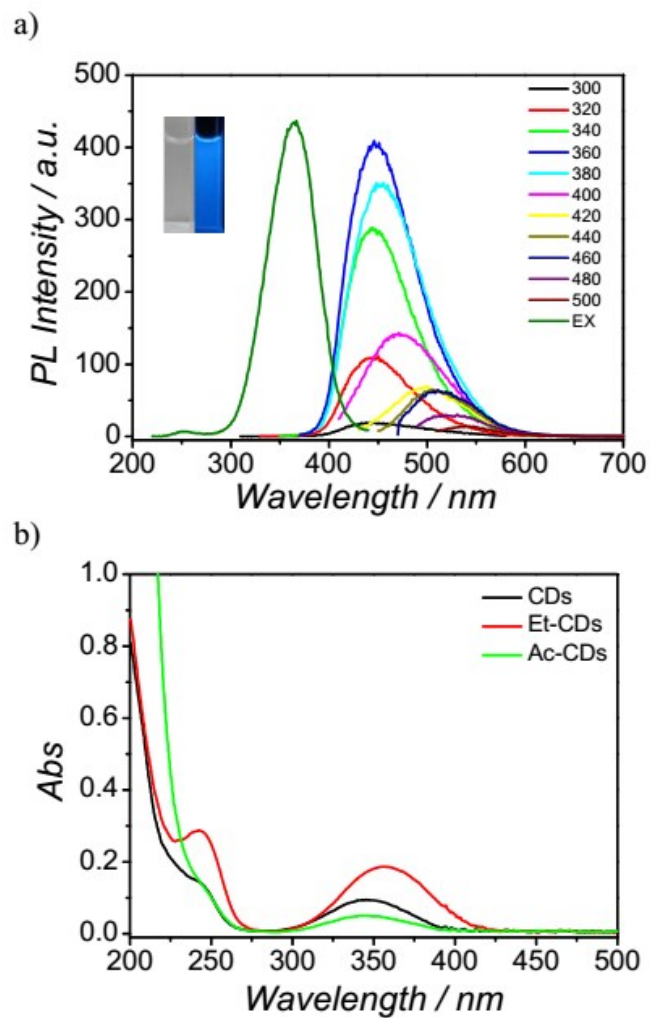


Figure S7 The PL and Abs spectra of modified CDs a) PL spectra of Ac-CDs inset: photographs of Ac-CDs solution under visible and UV light and b) the Abs spectra of three kinds of CDs.

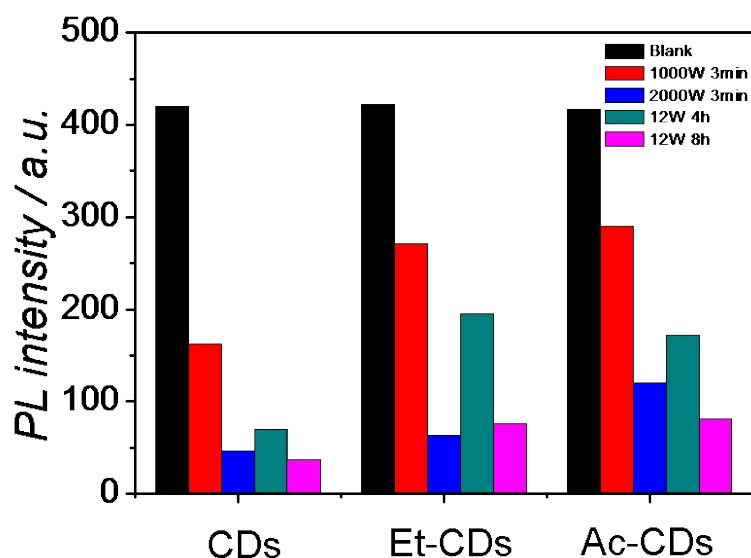


Figure S8 PL stability of modified CDs. The different kinds of CDs were synthesized at 140 °C. The concentration of CDs was around 0.01 mg/mL. The PL intensity of these three CDs was tuned at the same level. CDs were exposure either strong UV light (1000 W and 2000 W) or weak UV light (handy UV lamp 12W).

Note: The photostability was much improved since imine group was protected. Et-CDs were a kind of ideal fluorescent material, since they possessed high yield, quantum yield and high photo-stability. So as to Ac-CDs, the photostability of Ac-CDs was much improved, but the production yield and QY decreased dramatically.

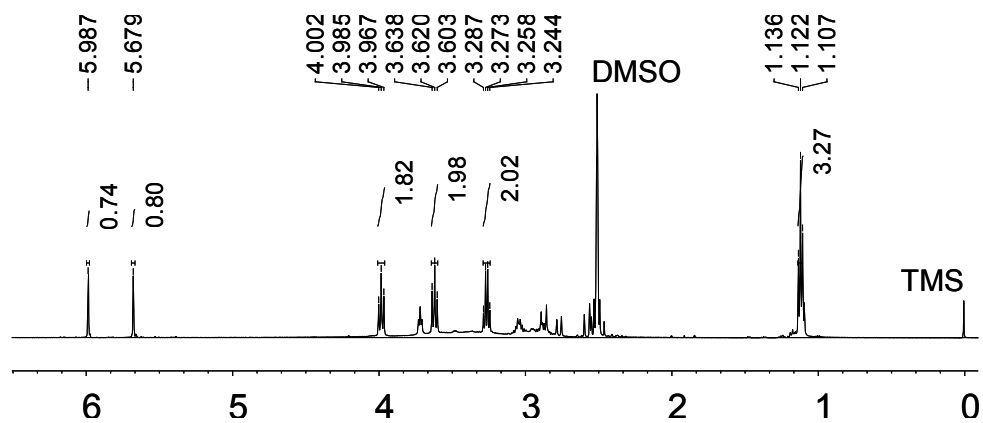


Figure S9 ¹H-NMR spectra of the Et-CDs.

Note: The marked NMR signal peaks were attributed to Et-IPCA (Figure 4d). Other peaks (2.5-3.8 ppm) were attributed to the by-product in Et-CDs.

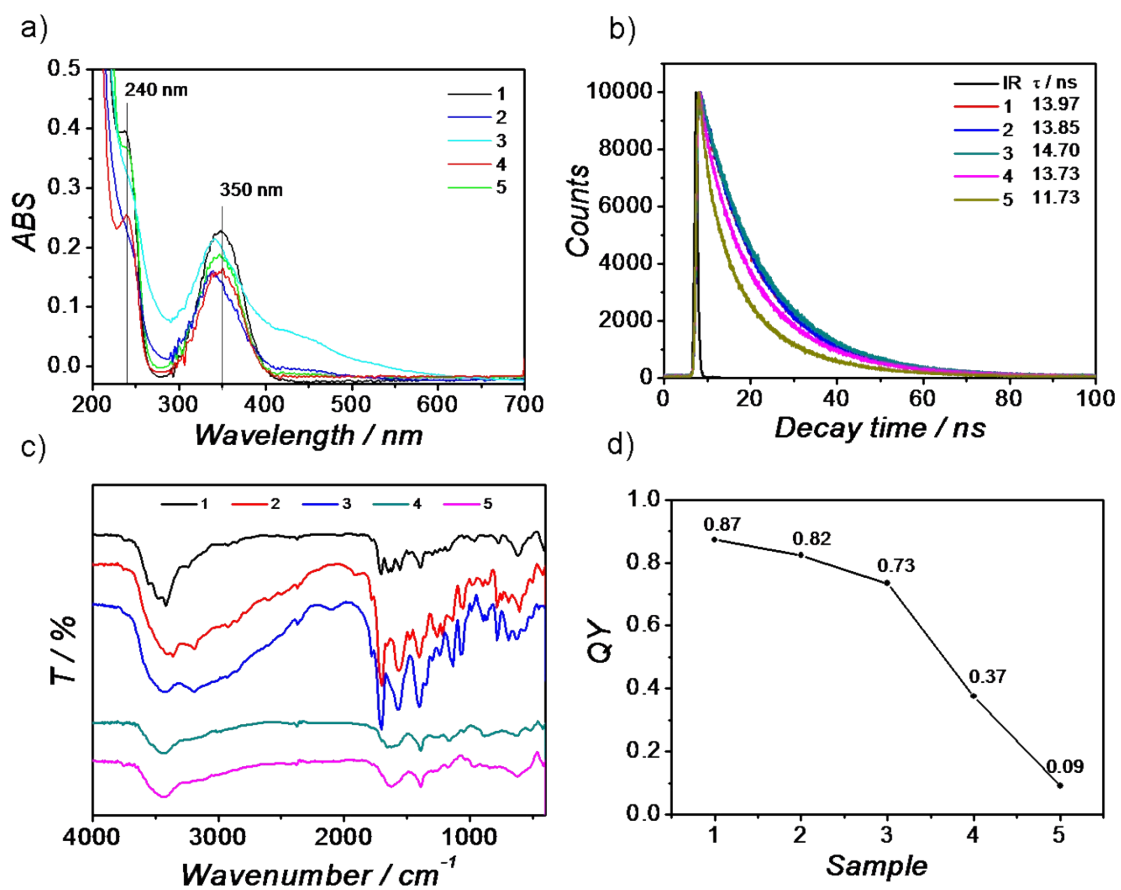


Figure S10 Characterization of 5 batches from column chromatography: a) Absorbance, b) PL lifetime, c) IR spectra, d) PL QY.

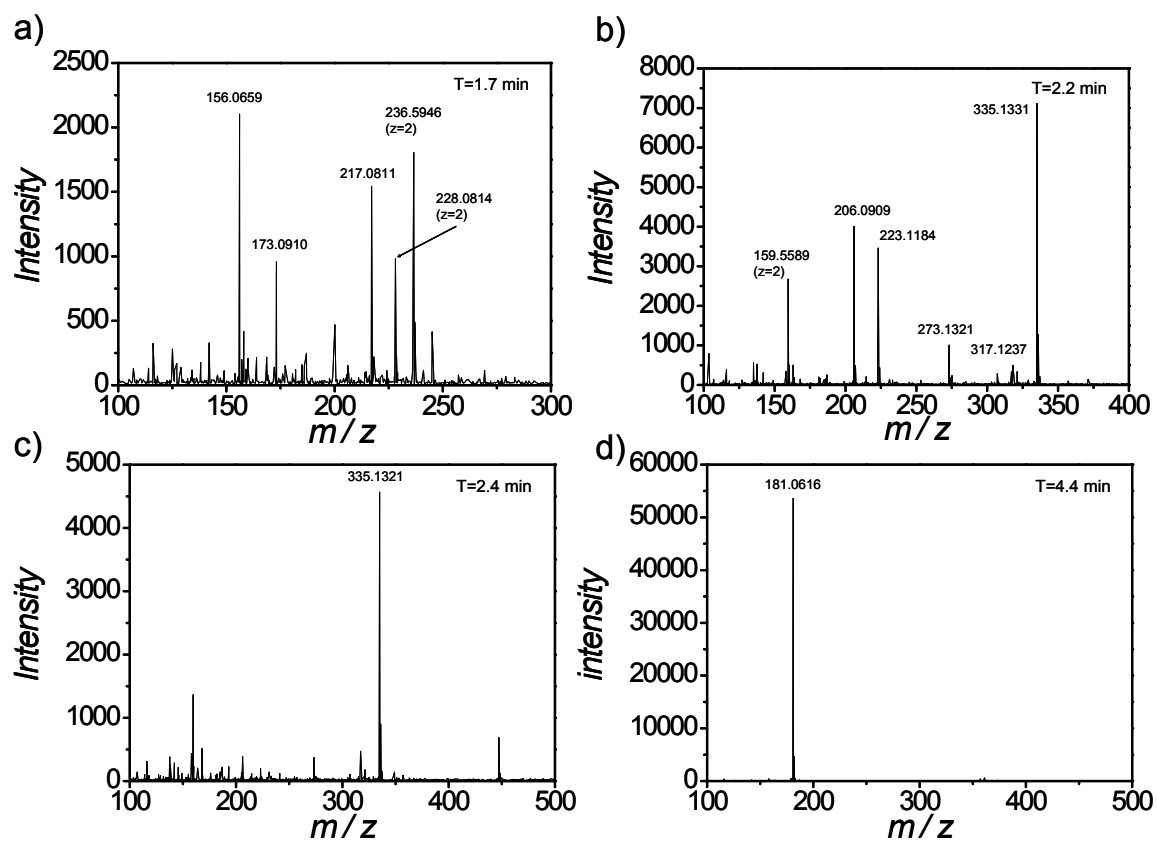


Figure S11 High resolution mass spectra of CDs-140 of different retention time.

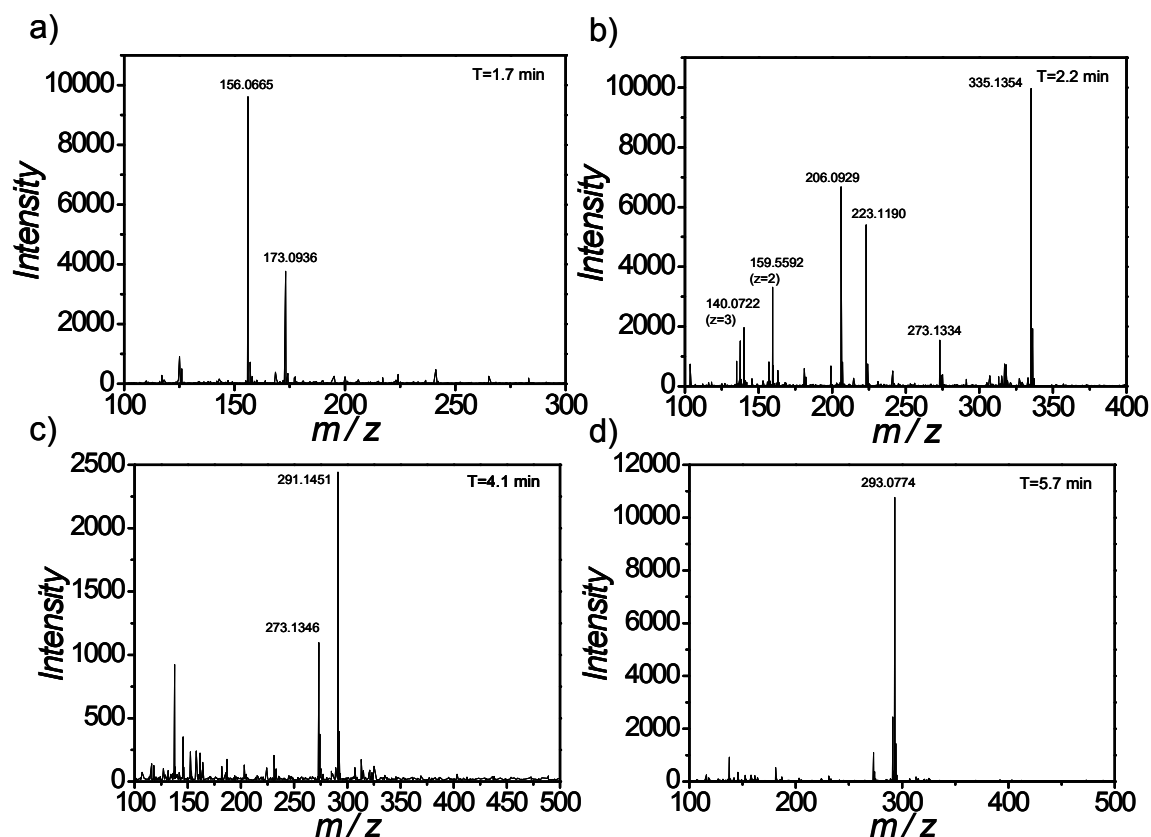


Figure S12 High resolution mass spectra of CDs-200 of different retention time. (Spectra of 4.4 min was in Figure 6)

Note: 1) The analysis results table of LC-MS mass spectra

Substance	MW	Chemical formula	Possible structure
Dimer	156	$C_7H_{10}NO_3^+$	CA+EDA-CO ₂ -NH ₃ -2H ₂ O+H ⁺
Dimer	173	$C_7H_{13}N_2O_3^+$	CA+EDA-CO ₂ -2H ₂ O+H ⁺
Dimer	181	$C_8H_9N_2O_3^+$	CA+EDA-4H ₂ O+H ⁺
Trimer	206	$C_{10}H_{12}N_3O_2^+$	CA+2EDA-NH ₃ -5H ₂ O+H ⁺
Dimer	217	$C_8H_{13}N_2O_5^+$	CA+EDA-2H ₂ O+H ⁺
Trimer	223	$C_{10}H_{15}N_4O_2^+$	CA+2EDA-5H ₂ O+H ⁺
Tetramer	273	$C_{14}H_{17}N_4O_2^+$	2CA+2EDA-2CO ₂ -8H ₂ O+H ⁺
Tetramer	317	$C_{15}H_{17}N_4O_4^+$	2CA+2EDA-CO ₂ -8H ₂ O+H ⁺
Tetramer	335	$C_{15}H_{19}N_4O_5^+$	2CA+2EDA-CO ₂ -7H ₂ O+H ⁺
3*Dimer	228	$C_{22}H_{24}N_4O_7^{2+}$	3CA+3EDA-2CO ₂ -2NH ₃ -10H ₂ O+2H ⁺
3*Dimer	236.5	$C_{22}H_{27}N_5O_7^{2+}$	3CA+3EDA-2CO ₂ -NH ₃ -10H ₂ O+2H ⁺

2) The mass spectra were calibrated by sodium formate as internal label, and the deviation was not more than 3 mDa. 3) Isomerism may exist in these compounds, so the specific chemical structure was not predicted. 4) In fact, the result of CDs-140 and CDs-200 were almost the same, but CDs-140 contained more components in short retention time and CDs-200 contained more components in longer retention time.

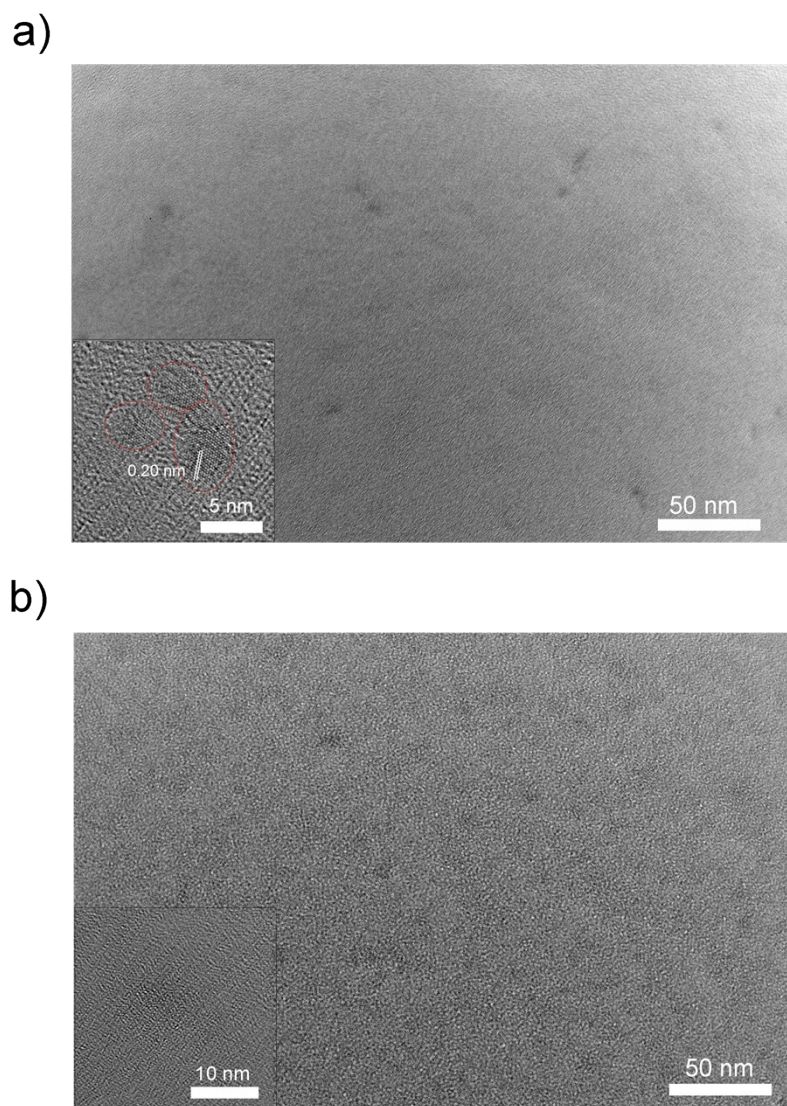


Figure S13 The TEM image of batch 4 a) and batch 5 b) of the CDs. Insert: HRTEM of the CDs.

Note: Some CDs possessed the crystal lattice, which was like that of graphite, and some CDs were amorphous. Due to the low contrast ratio, amorphous CDs were hard to be observed. There were more CDs with crystal lattice in batch 4 than in batch 5.

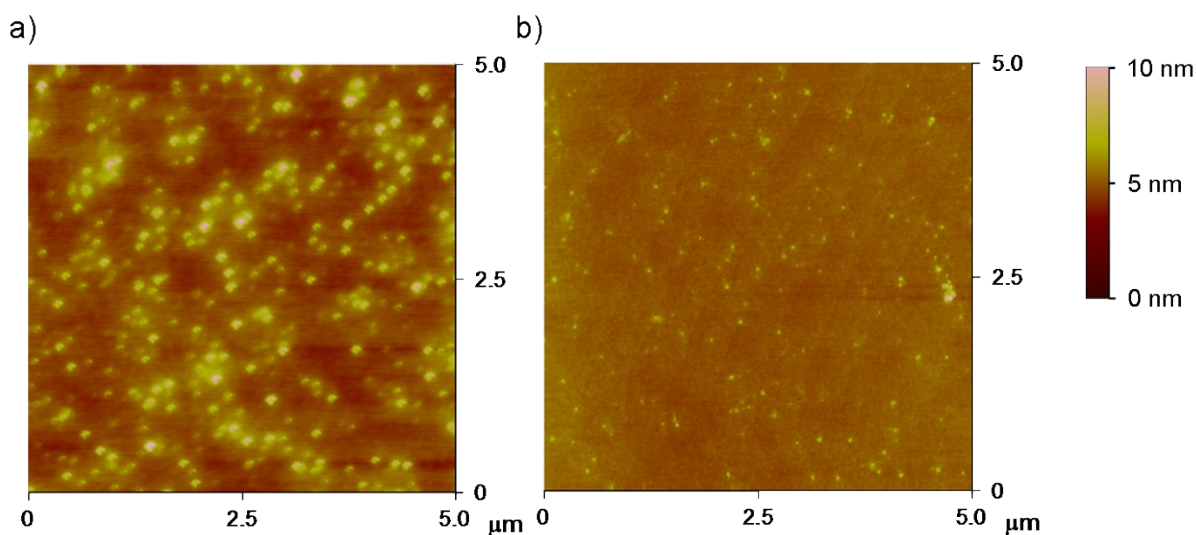


Figure S14 AFM image of the batch 4 of CDs. The samples were prepared by spin coating aqueous solution of carbon core on mica plate. a) concentrated solution b) diluted solution after ultrasonic processing. The average height of b) sample was 1.26 ± 0.40 nm.

Note: The actually size of carbon core are around 2-6 nm according to our previous work¹ and it can also be approved by the TEM image in figure S13. The actual diameter of CDs may be larger than their height on the substrate. We suspected the carbon core was soft layered structure rather than solid spherical on the substrate. On one hand the so called carbon core may contain soft polymer structure, and it will collapse and spread on the substrate without evaporation of the solvent. On the other hand, graphene like structure may form through of pyrolysis citric acid².

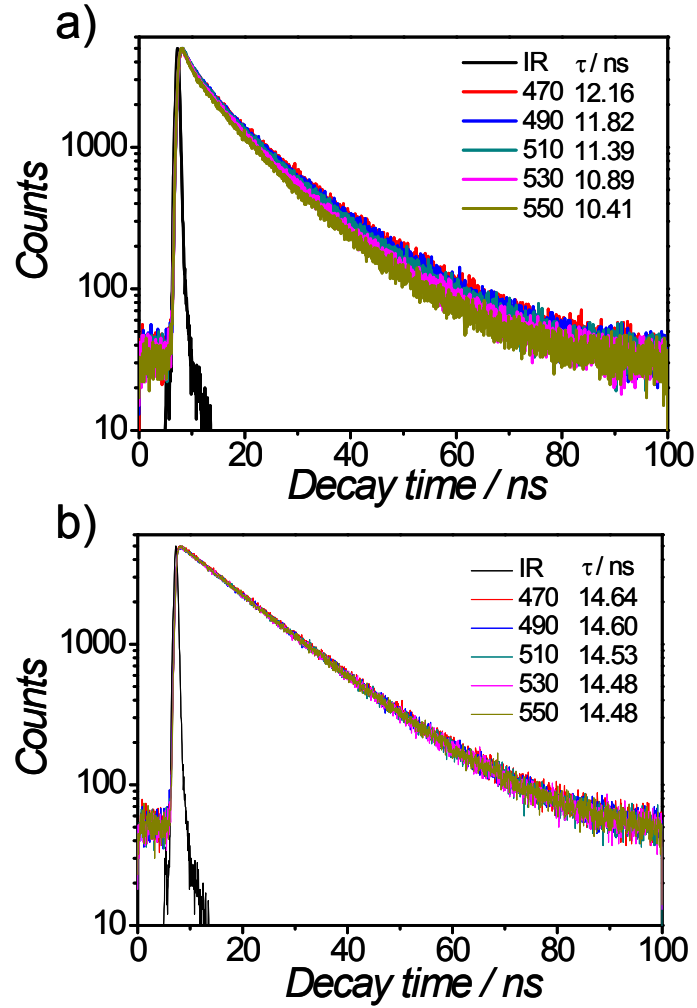


Figure S15 The PL lifetime measurement of batch 1 a) and batch 4 b). The PL excitation was 360 nm while the PL received position changed from 470 nm to 550 nm.

Note: The PL intensity decay tendency followed single exponential for batch 1 and it kept consistent for different detected wavelength. The PL lifetime of batch 4 was comprised of two parts and the average PL lifetime changed as the emission wavelength changed. The PL intensity decay tendency followed double exponential for batch 4. The fitting lifetimes were listed in the table below.

Wavelength[nm]	τ_1 [ns]	n1 [%]	τ_2 [ns]	n2 [%]	τ_{aver} [ns]
470	3.76	18.91	14.12	81.09	12.16
490	3.57	18.53	13.70	81.47	11.82
510	3.44	18.70	13.22	81.30	11.39
530	3.32	19.22	12.69	80.78	10.89
550	2.84	17.66	12.03	82.34	10.41

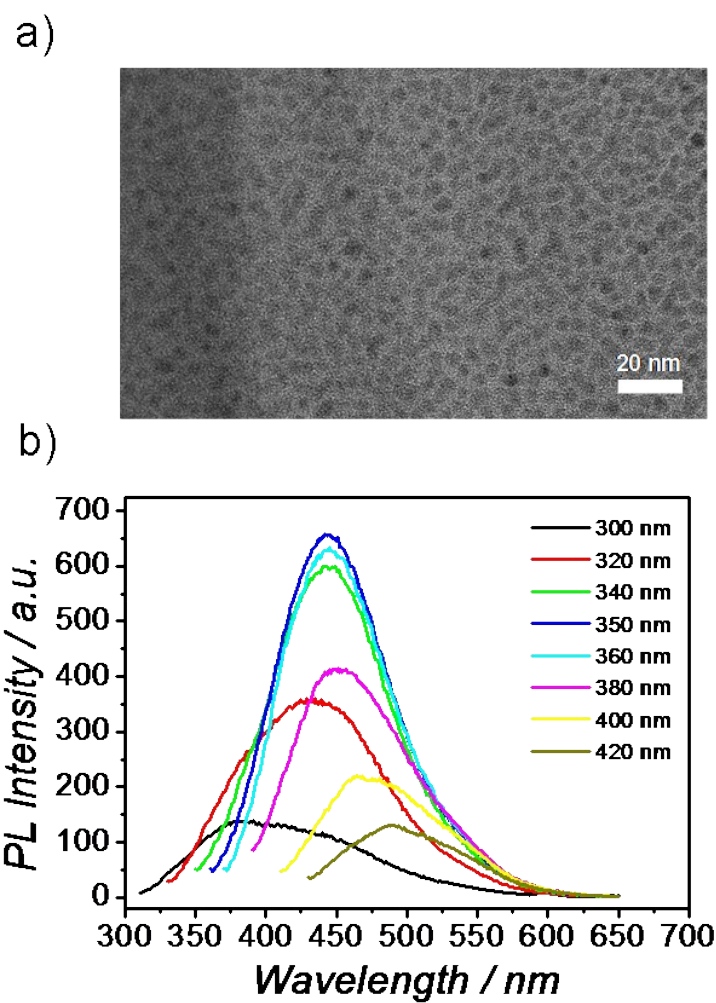


Figure S16 The TEM image a) and PL spectra b) of carbon core made from hydrothermal treatment of CA at 200°C.

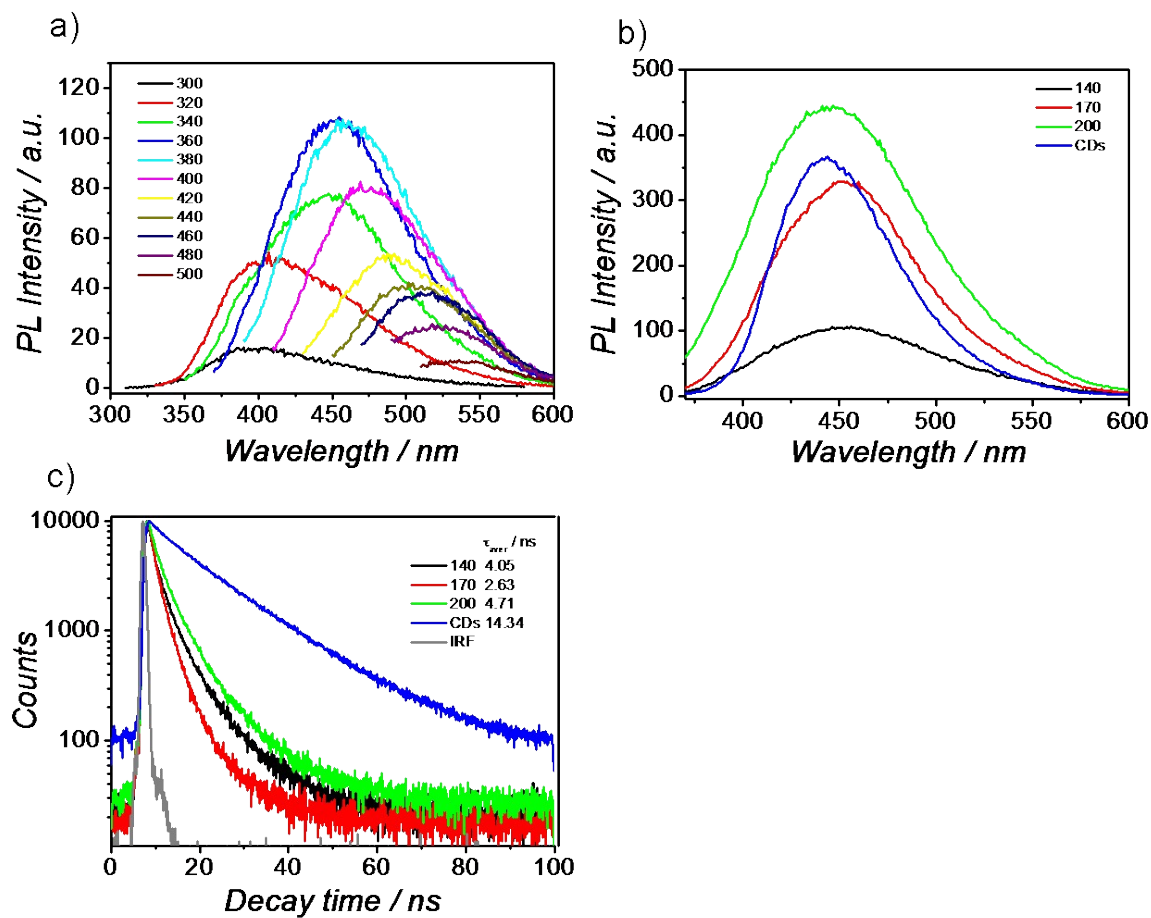


Figure S17. The PL and PL lifetime characterization of carbon core. a) PL spectra of carbon core made from hydrothermal treatment of CA at 140°C (carbon core-140). b) The PL intensity comparison of carbon core-140, carbon core-170, carbon core-200 and CDs. c) The PL lifetime measurement of carbon cores and CDs.

Note: In figure S17b, the concentration of carbon core was around 100 mg/mL (no dilution) and the concentration of CDs was ca. 0.001 mg/mL. In figure S17c, the excitation wavelength was 370 nm and the emission wavelength was 450 nm.

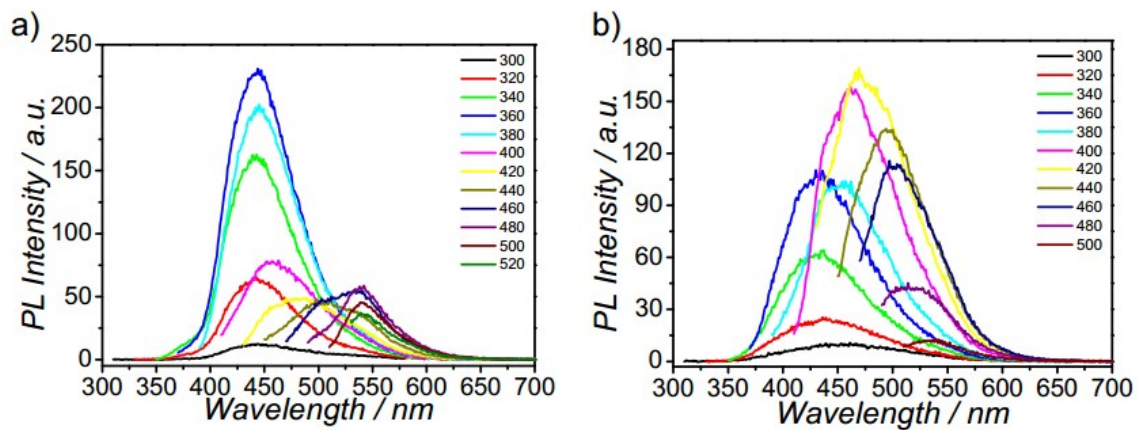


Figure S18 The PL spectra of IPCA after hydrothermal treatment. a) 140 °C, 10 h, the QY was 36% b) 200 °C, 10 h, the QY was 16%.

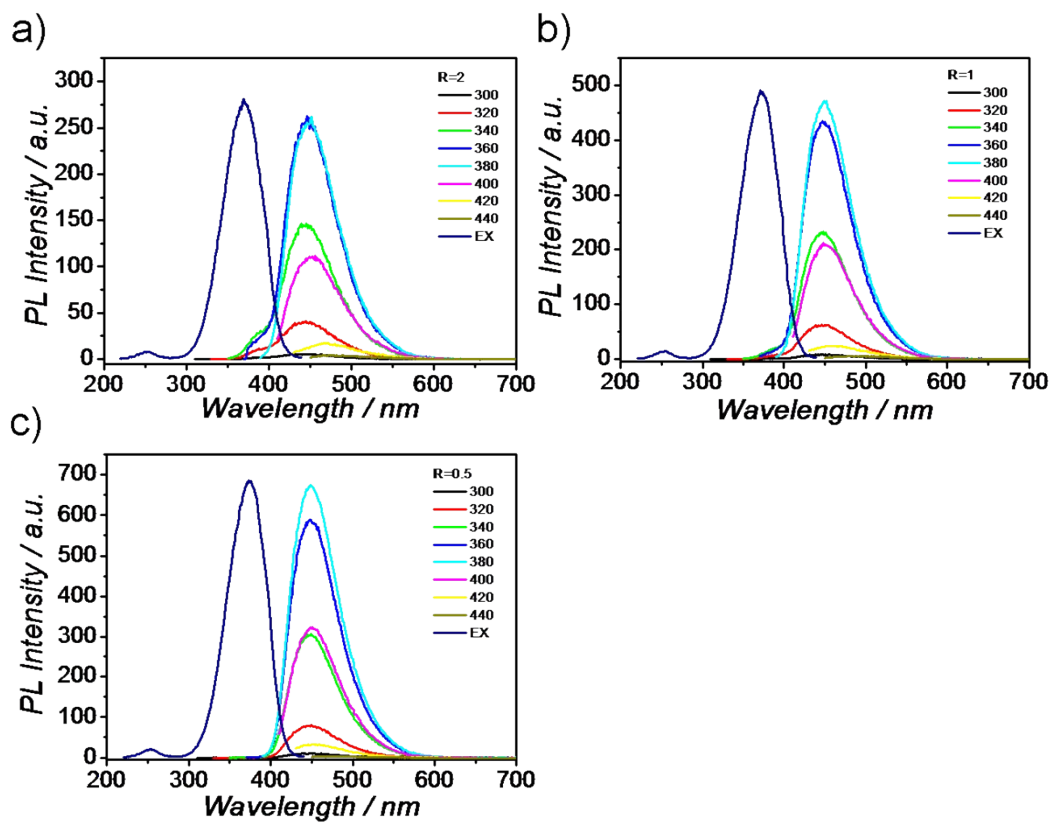


Figure S19 PL spectra of Et-CDs solution synthesized in 200°C condition. The ratio of CA and Et-EDA (R) was different: a) the R was 2, b) the R was 1, c) the R was 0.5.

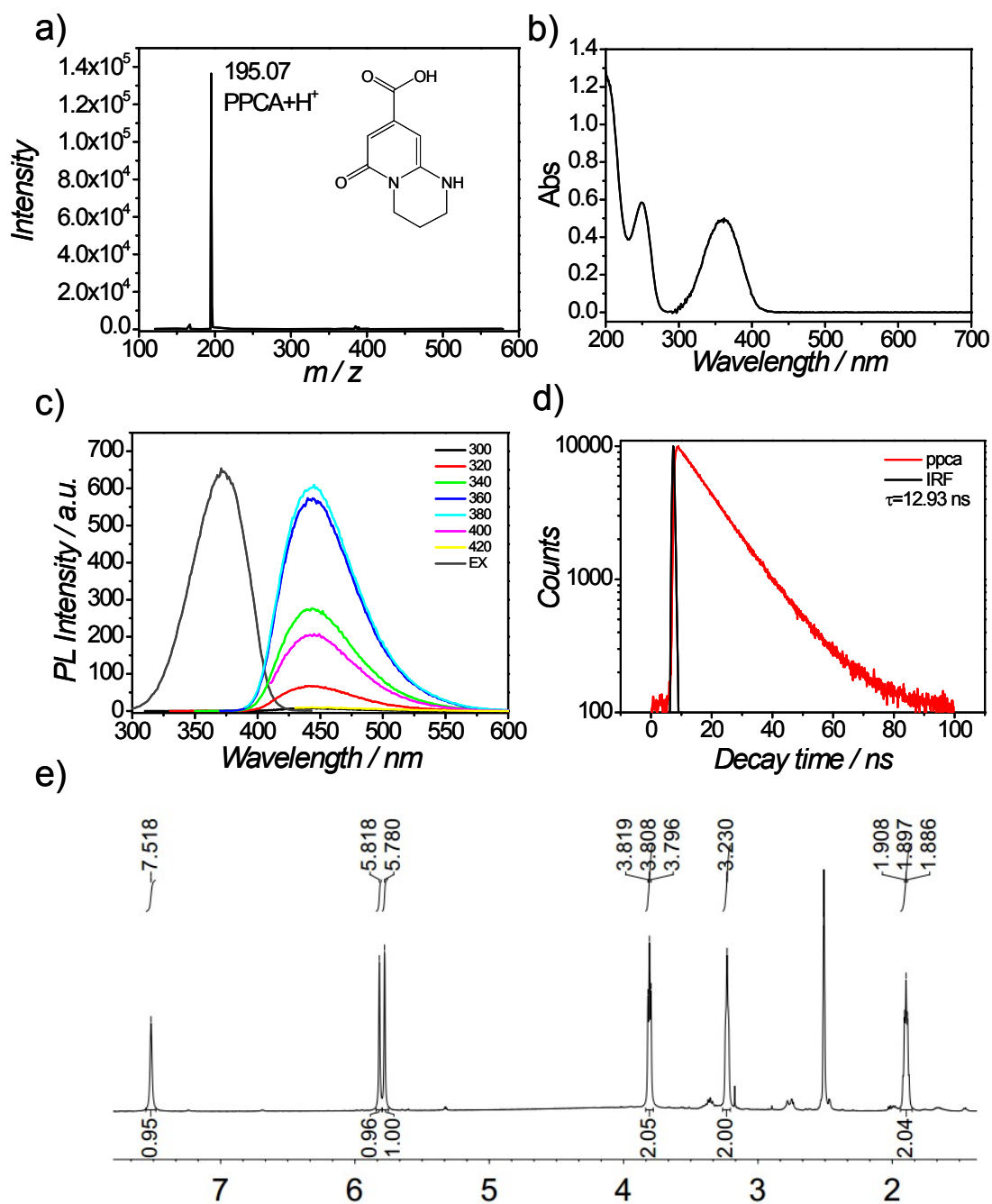


Figure S20

The characterization of 6-oxo-2,3,4,6-tetrahydro-1H-pyrido[1,2-a]pyrimidine-8-carboxylic acid (PPCA): a) The structure of PPCA and ESI mass spectrum, b) Absorbance spectrum, c) PL spectra d) PL lifetime measurement and e) ¹H-NMR spectrum.

Bio-application of IPCA

Human islet amyloid polypeptide (hIAPP) or amylin is a 37-residue peptide hormone, which is co-secreted with insulin. hIAPP has a strong amyloidogenic propensity, which is toxic to cultured islet β -cells and contribute to the pathology of type II diabetics.³⁻⁴ Many types of aggregation inhibitors, including single molecule, peptide and nanosized materials showed talent in inhibition of amyloid fibril formation.⁵⁻⁷ We found IPCA can inhibit hIAPP amyloid fibrils formation, which was proved by the Thioflavin-T (ThT) fluorescence assay, TEM test and cell toxicity assays. When in the absence of IPCA, the ThT-binding assay gave strong ThT emissions at 484 nm and the following TEM data suggested that hIAPP formed typical long linear fibrils (Figure S21). The group with equimolar amounts of IPCA exhibited strong inhibition on the ThT emission (Figure S21a) and less amyloid fibrils in TEM image (Figure S21d). In cell toxicity assays, IPCA can increase the livability of the cells (Figure S21b), because IPCA can reduce the amount of amyloid fibrils, which are harmful to cells. IPCA showed obvious anti-amyloid functions and hold the potential as a facile biological agent.

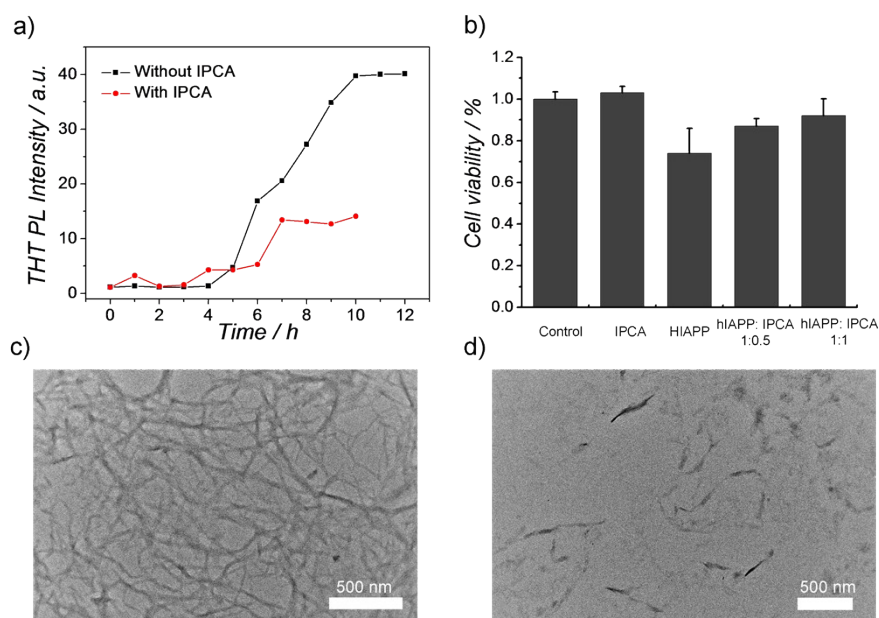


Figure S21. The aggregation behaviors of hIAPP in PBS (pH 7.4) buffer solution with and without adding IPCA. a) ThT monitored kinetic process of aggregation for hIAPP alone and 1:1 (weight ratio) mixture of hIAPP and IPCA. b) Cell viability of INS-1 cells treated with hIAPP in the absence and presence of IPCA. c) and d) The TEM images of hIAPP after 48 h incubation in the absence and presence of IPCA, respectively.

Experiment details: The Thioflavin-T fluorescence assays were performed on a fluorescence spectrophotometer RF-5301 PC using a 450 nm excitation filter and a 484 nm emission filter. The assays were started immediately after diluting hIAPP solution freshly prepared in 60 μ L ultrapure water at 4 $^{\circ}$ C in the absence and presence of IPCA and then addition of PBS buffer solution. The concentrations of hIAPP and ThT were 15 μ M and 20 μ M respectively. TEM images were acquired on JEM-2100F transmission electron microscope. 5 μ L solution for ThT assays were spotted on a 300-mesh Formvar-carbon coated copper grid for 2 min. After washed twice with 10 μ L ultrapure water, the sample were air-dried overnight and stained with 1% freshly prepared uranyl formate. Images were recorded on TEM with an accelerating voltage of 200 kV.

Cell toxicity assays were achieved using INS-1 cells. The cells were grown in RPMI-1640 supplemented with 10% (v/v) FBS, 50 U/mL penicillin, 50 μ g/mL streptomycin and 50

$\mu\text{mol/L}$ 2-mercaptoethanol. Cells were seeded in 96-well plate at a density of 1×10^4 cells per well and incubated at 37°C in 5% CO_2 atmosphere for 24 h. The media were replaced with fresh media with 0.06 mg/mL hIAPP and/or 0.06/0.03 mg/mL IPCA. Following 20 h incubation, 15 μL MTT were added to each well and incubated for another 4 h. The absorbance was measured by a microplate spectrometer reader at 540 nm.

References in ESI

1. S. Zhu, Q. Meng, L. Wang, J. Zhang, Y. Song, H. Jin, K. Zhang, H. Sun, H. Wang and B. Yang, *Angew. Chem. Int. Ed.*, 2013, **52**, 3953-3957.
2. Y. Q. Dong, J. W. Shao, C. Q. Chen, H. Li, R. X. Wang, Y. W. Chi, X. M. Lin and G. N. Chen, *Carbon*, 2012, **50**, 4738-4743.
3. A. E. Butler, J. Janson, S. Bonner-Weir, R. Ritzel, R. A. Rizza and P. C. Butler, *Diabetes*, 2003, **52**, 102-110.
4. F. Chiti and C. M. Dobson, *Annu. Rev. Biochem.* 2006, **75**, 333-366.
5. R. Mishra, B. Bulic, D. Sellin, S. Jha, H. Waldmann and R. Winter, *Angew. Chem. Int. Ed.*, 2008, **47**, 4679-4682.
6. L. Wang, L. Lei, Y. Li, L. Wang and F. Li, *FEBS letters*, 2014, **588**, 884-891.
7. M. Zhang, X. Mao, Y. Yu, C. X. Wang, Y. L. Yang and C. Wang, *Adv. Mater.*, 2013, **25**, 3780-3801.